Why two clocks synchronize: Energy balance of the synchronized clocks

Krzysztof Czołczyński, Przemysław Perlikowski, Andrzej Stefański, and Tomasz Kapitaniak
Division of Dynamics, Technical University of Lodz, Stefanowskiego 1/15, 90-924 Lodz, Poland

(Received 27 February 2011; accepted 2 June 2011; published online 24 June 2011)

We consider the synchronization of two clocks which are accurate (show the same time) but have pendulums with different masses. We show that such clocks hanging on the same beam beside the complete (in-phase) and antiphase synchronizations perform the third type of synchronization in which the difference of the pendulums' displacements is a periodic function of time. We identify this period to be a few times larger than the period of pendulums' oscillations in the case when the beam is at rest. Our approximate analytical analysis allows to derive the synchronizations conditions, explains the observed types of synchronizations, and gives the approximate formula for both the pendulums' amplitudes and the phase shift between them. We consider the energy balance in the system and show how the energy is transferred between pendulums via oscillating beam allowing pendulums' synchronization. © *2011 American Institute of Physics*. [doi:10.1063/1.3602225]

Synchronization in coupled dynamical systems is associated with the emergence of collective coherent behavior between identical or similar subsystems. The first reported observation of this phenomenon is the Huygens' pendulum clocks experiment in which antiphase synchronization of clocks' pendulums has been observed. An important step in understanding of the synchronization is to identify how the energy is transferred between the subsystems. Based on the energy balance we derive approximate analytical formulas which explain both in-phase and antiphase synchronization of the clocks. Additionally, we show the possibility of the long period generalized synchronization and chaotic behavior of the pendulums.

I. INTRODUCTION

In 1665, C. Huygens noticed the antiphase synchronization of two pendulum clocks mounted together on the same beam (Huygens, 1665). This was one of the first observations of the phenomenon of the coupled harmonic oscillators, which have many applications in physics (Pikovsky *et al*., 2001; Blekham, 1988). Recently, this idea has been rediscussed by a few groups of researchers who tested Huygens' idea (Pogromsky *et al*., 2003; Bennet *et al*., 2002; Senator, 2006; Dilao, 2009; Kumon *et al*., 2002; Fradkov and Andrievsky, 2007; Pantaleone, 2002; Ulrichs *et al*., 2009; Czolczynski *et al*., 2009a). To explain Huygens' observations, special experimental devices have been built. One of them (Bennet *et al*., 2002) consists of two interacting pendulum clocks hanged on a heavy support which was mounted on a low-friction wheeled cart. The device moves by the action of the reaction forces generated by the swing of two pendulums and the interaction of the clocks occurs due to the motion of the clocks' base. It has been shown that to repeat Huygens' results, high precision (the precision that Huygens certainly could not achieve) is necessary. Another device, the so-called "coupled pendulums of the Kumamoto University" (Kumon *et al*., 2002), consists of two pendulums which suspension rods are connected by a weak spring, and one of the pendulums is excited by an external rotor. The numerical results of Fradkov and Andrievsky (2007) show simultaneous approximate in-phase and anti-phase synchronization. Both types of synchronization can be obtained for different initial conditions. Additionally, it has been shown that for small difference in the pendulums' frequencies they may not synchronize. Finally, in Czolczynski *et al*. (in press), it has been shown that two real mechanical clocks when mounted to the horizontally moving beam can synchronize both in phase and antiphase.

In this paper, we consider the synchronization of two clocks which have pendulums with the same length but different masses. Such clocks are accurate, i.e., show the same time as both pendulums have the same length. We show that two such clocks hanging on the same beam beside the complete (in-phase) and antiphase synchronizations already demonstrated in Blekham (1988), Bennet *et al*. (2002), and Czolczynski *et al*. (in press) perform the third type of synchronization in which the difference of the pendulums' displacements φ_1-φ_2 is a periodic function of time. We identify this period to be larger than the period of pendulums' oscillations in the case when beam M is at rest. This type of generalized synchronization has been called a *long period synchronization*. We perform an approximate analytical analysis, which allows deriving the synchronizations conditions, explains observed types of synchronizations, and gives approximate formula for both the pendulums' amplitudes and phase shift between them. The energy balance in the system allows to show how the energy is transferred between the pendulums via the oscillating beam. Additionally, we show that beside the periodic synchronous behavior clocks' pendulums can perform chaotic oscillations.

This paper is organized as follows. Section II describes the model of the clocks which has been used. In Sec. III, we derive the energy balance of the synchronized pendulums. Section IV presents the results of our numerical simulations, describes the observed synchronizations states together with the energy balance of the pendulums. Finally, we summarize our results in Sec. V.

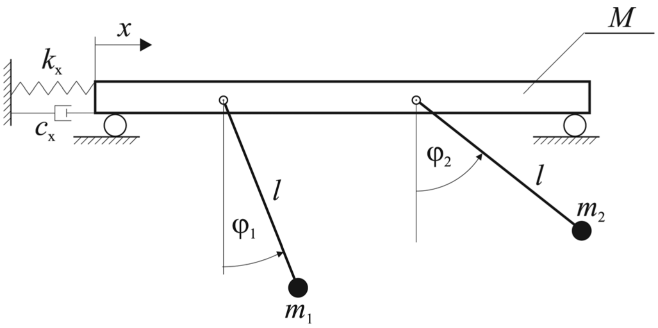

FIG. 1. The model of the system – two pendulum clocks are mounted to the beam which can move horizontally.

II. MODEL

The analyzed system is shown in Figure 1; it consists of the rigid beam and two pendulum clocks suspended on it. The beam of mass M can move in a horizontal direction, and its movement is described by coordinate x. The mass of the beam is connected to the refuge of a linear spring and linear damper k_x and c_x. Clocks' pendulum consists of the light beam of the length l and mass mounted at its end. We consider the pendulums with the same length l but different masses m_1 and m_2. The same length of both pendulums guarantee that the clocks are accurate, i.e., both show the same time. The motion of the pendulums is described by angles φ_1 and φ_2 and is damped by dampers (not shown in Figure 1) with damping coefficients $c_{\varphi 1}$ and $c_{\varphi 2}$. The damping coefficients $c_{\varphi 1,2}$ are proportional to the pendulums' masses $m_{1,2}$. This proportionality causes that in the lack of forcing (when the clock is not winded), the oscillations of both pendulums decay with the same speed. The pendulums are driven by the escapement mechanism described in details in Huygens (1673), Rowlings (1944), Lepschy *et al.* (1993), Roup *et al.* (2003), Moon and Stiefel (2006), and Czolczynski *et al.* (2009b). Notice that when the swinging pendulums do not exceed certain angle γ_N, the escapement mechanisms generate the constant moments M_{N1} and M_{N2} (proportional to the pendulum masses $m_{1,2}$).

This mechanism acts in two successive steps, i.e., the first step is followed by the second one and the second one by the first one (the detailed description of the escapement mechanism has been given in our previous work (Czolczynski *et al.*, 2009b)). In the first step if $0 < \varphi_i < \gamma_N$ $(i = 1,2)$, then $M_{Di} = M_{Ni}$ and when $\varphi_i < 0$, then $M_{Di} = 0$. For the second stage, one has for $-\gamma_N < \varphi_i < 0$ $M_{Di} = -M_{Ni}$ and for $\varphi_i > 0$, $M_{Di} = 0$. The energy supplied by the escapement mechanic balance the energy dissipated due to the damping. The parameters of this mechanics have been chosen in the way that for the beam M at rest both pendulums perform oscillations with the same amplitude. Typically for pendulum clocks that oscillate with amplitude smaller then $2\pi/36$ and for clocks with long pendulums like marine clocks, this amplitude is even smaller (Rowlings, 1944).

The equations of motion are as follows:

$$m_i l^2 \ddot{\varphi}_i + m_i \ddot{x} l \cos\varphi_i + c_{\varphi i}\dot{\varphi}_i + m_i g l \sin\varphi_i = M_{Di}\,, \tag{1}$$

$$\left(M + \sum_{i=1}^{2} m_i\right)\ddot{x} + c_x\dot{x} + k_x x + \sum_{i=1}^{2} m_i l \times \left(\ddot{\varphi}_i \cos\varphi_i - \dot{\varphi}_i^2 \sin\varphi_i\right) = 0, \tag{2}$$

$i = 1,2$. Equations (1) and (2) describes the dynamical system which performs the self-excited oscillations (Andronov *et al.*, 1966).

Clocks are designed in such a way that the pendulums perform periodic motion with a period $2\pi/\alpha$ where α is constant. The escapement mechanism provides the necessary amount of energy to compensate the dissipation and makes the pendulum motion periodic. Under these assumption in the state of phase or antiphase synchronization, the motion of the clock's pendulums has been approximated by

$$\varphi_i = \Phi_i \sin(\alpha t + \beta_i), \tag{3}$$

and

$$\begin{aligned}\dot{\varphi}_i &= \alpha\Phi_i \cos(\alpha t + \beta_i),\\ \ddot{\varphi}_i &= -\alpha^2\Phi_i \sin(\alpha t + \beta_i).\end{aligned} \tag{4}$$

Our numerical simulations show that continuous solution given by Eq. (3) is a good approximation of the pendulums' oscillations calculated from discontinuous Eqs. (1) and (2) in the case of both identical and nonidentical clocks. Substituting Eqs. (3) and (4) into Eq. (2) one gets

$$\begin{aligned}&\left(M + \sum_{i=1}^{2} m_i\right)\ddot{x} + c_x\dot{x} + k_x x\\ &\quad = \sum_{i=1}^{2}\big(m_i l\alpha^2\Phi_i \sin(\alpha t + \beta_i) + m_i l\alpha^2\Phi_i^3\\ &\qquad \times \cos^2(\alpha t + \beta_i)\sin(\alpha t + \beta_i)\big).\end{aligned} \tag{5}$$

Considering $\cos^2\alpha \sin\alpha = 0.25 \sin\alpha + 0.25 \sin 3\alpha$, and denoting

$$\begin{aligned}&U = M + \sum_{i=1}^{2} m_i, \quad F_{1i} = m_i l\alpha^2(\Phi_i + 0.25\Phi_i^3),\\ &F_{3i} = 0.25 m_i l\alpha^2\Phi_i^3,\end{aligned} \tag{6}$$

we have

$$U\ddot{x} + c_x\dot{x} + k_x x = \sum_{i=1}^{2}\left(F_{1i}\sin(\alpha t + \beta_i) + F_{3i}\sin(3\alpha t + 3\beta_i)\right). \tag{7}$$

Assuming the small value of the damping coefficient c_x, Eq. (7) can be rewritten in the following form:

$$x = \sum_{i=1}^{2}\left(X_{1i}\sin(\alpha t + \beta_i) + X_{3i}\sin(3\alpha t + 3\beta_i)\right), \tag{8}$$

where

$$\begin{aligned}X_{1i} &= \frac{F_{1i}}{k_x - \alpha^2 U} = \frac{m_i l\alpha^2(\Phi_i + 0.25\Phi_i^3)}{k_x - \alpha^2 U},\\ X_{3i} &= \frac{F_{3i}}{k_x - 9\alpha^2 U} = \frac{0.25 m_i l\alpha^2\Phi_i^3}{k_x - 9\alpha^2 U}.\end{aligned} \tag{9}$$

Equation (7) implies the following acceleration of the beam M:

$$\ddot{x} = \sum_{i=1}^{2}\left(A_{1i}\sin(\alpha t + \beta_i) + A_{3i}\sin(3\alpha t + 3\beta_i)\right), \tag{10}$$

where

$$A_{1i} = -\frac{m_i l \alpha^4 (\Phi_i + 0.25\Phi_i^3)}{k_x - \alpha^2 U},$$
$$A_{3i} = -\frac{0.25 m_i l \alpha^4 \Phi_i^3}{k_x - 9\alpha^2 U}. \tag{11}$$

Notice that Eq. (11) consists of the first and third harmonic components only.

III. ENERGY BALANCE OF THE CLOCKS' PENDULUMS

Multiplication of both sides of Eq. (1) by the angular velocity of the i-th pendulum gives

$$m_i l^2 \ddot{\varphi}_i \dot{\varphi}_i + m_i g l \dot{\varphi}_i \sin\varphi_i = M_{Di}\dot{\varphi}_i - c_{\varphi i}\dot{\varphi}_i^2 - m_i \ddot{x} l \cos\varphi_i \dot{\varphi}_i. \tag{12}$$

In the case of the periodic motion of the pendulums after integration, Eq. (12) gives the energy balance of the i-th pendulum

$$\int_0^T m_i l^2 \ddot{\varphi}_i \dot{\varphi}_i dt + \int_0^T m_i g l \dot{\varphi}_i \sin\varphi_i dt = \int_0^T M_{Di}\dot{\varphi}_i dt - \int_0^T c_{\varphi i}\dot{\varphi}_i^2 dt - \int_0^T m_i \ddot{x} l \cos\varphi_i \dot{\varphi}_i dt. \tag{13}$$

The left hand side of Eq. (13) represents the decrease of the total energy of the i-th pendulum. In the case of the periodic behavior of the system (1,2), this decrease is equal to zero, so

$$\int_0^T m_i l^2 \ddot{\varphi}_i \dot{\varphi}_i dt + \int_0^T m_i g l \dot{\varphi}_i \sin\varphi_i dt = 0. \tag{14}$$

The work done by the escapement mechanism during tone period of pendulum's oscillations can be expressed as

$$W_i^{DRIV} = \int_0^T M_{Di}\dot{\varphi}_i dt = 2\int_0^{\gamma_N} M_{Ni} d\varphi_i = 2M_{Ni}\gamma_N. \tag{15}$$

As we have already assumed this work is proportional to the mass of the pendulum and does not depend on the pendulum's displacement $\varphi_{1,2}$ ($\varphi_{1,2} > \gamma_N$) and velocity. Energy dissipated in the damper is given by

$$W_i^{DAMP} = \int_0^T c_{\varphi i}\dot{\varphi}_i^2 dt = \int_0^T c_{\varphi i}\alpha^2\Phi_i^2 \cos^2(\alpha t + \beta_i) dt = \pi\alpha c_{\varphi i}\Phi_i^2. \tag{16}$$

(In the integration we used Eq. (4) and the relation $\int_0^T \cos\alpha t \cos\alpha t dt = 0.5\ T = \frac{\pi}{\alpha}$.)

The last component of Eq.(13) represents the energy transferred from the i-th pendulum to the beam M (pendulum looses part of its energy to force the beam to oscillate), so we have

$$W_i^{SYN} = \int_0^T m_i \ddot{x} l \cos\varphi_i \dot{\varphi}_i dt. \tag{17}$$

Substituting Eqs. (15)–(17) into Eq.(13) one obtains energy balance for the i-th pendulum.

$$W_i^{DRIV} = W_i^{DAMP} + W_i^{SYN}. \tag{18}$$

Now let us consider the properties of Eq. (18) in a few special cases of the pendulums synchronization.

A. Energy balance during the anti-phase synchronization (identical pendulums)

In the case of the antiphase synchronization of two identical pendulums the beam M is in rest (Czolczynski *et al.*, 2009a,b). There is no energy transfer between pendulums and the beam so Eq. (18) has the form

$$W_i^{DRIV} = W_i^{DAMP}. \tag{19}$$

This balance for two clocks' pendulums is illustrated in Figure 6(a). Substituting Eqs. (15) and (16) into Eq. (19) one gets

$$2M_{Ni}\gamma_N = \pi\alpha c_{\varphi i}\Phi_i^2, \tag{20}$$

so one gets the expression

$$\Phi_i = \sqrt{\frac{2M_{Ni}\gamma_N}{\pi\alpha c_{\varphi i}}} \tag{21}$$

for the amplitude of the pendulum's oscillations.

B. Energy balance during the phase synchronization (pendulums with different masses)

In the case of two nonidentical clocks (with different pendulums masses) mounted to the beam M one can observe phase synchronization of the pendulums. The beam performs horizontal oscillations and the energy W_i^{SYN} is not equal zero. Substituting pendulum's velocity Eq. (4), beam's acceleration Eq. (10) into Eq. (18) and taking into account the simplification $\cos\varphi_i = 1.0$, one gets the expression for the energy transferred from i-th pendulum to the beam

$$W_i^{SYN} = \int_0^T (m_i l \ddot{x}\cos\varphi_i)\dot{\varphi}_i dt = \int_0^T m_i l \left(\sum_{j=1}^{2}\left(A_{1j}\sin(\alpha t + \beta_j) + A_{3j}\sin(3\alpha t + 3\beta_j)\right)\right) \times \alpha\Phi_i\cos(\alpha t + \beta_i)dt. \tag{22}$$

After further calculations one gets

$$W_i^{SYN} = m_i l \alpha \Phi_i \sum_{j=1}^{2} A_{1j}\frac{\pi}{\alpha}\left(-\cos\beta_j\sin\beta_i + \sin\beta_j\cos\beta_i\right) = m_i l\alpha\Phi_i \sum_{j=1}^{2} A_j \frac{\pi}{\alpha}\sin(\beta_j - \beta_i). \tag{23}$$

and after substitution of Eq. (11),

$$W_i^{SYN} = \frac{-m_i l^2\alpha^4\pi\Phi_i}{k_x - \alpha^2 U}\sum_{j=1}^{2} m_j(\Phi_j + 0.25\Phi_j^3)\sin(\beta_j - \beta_i). \tag{24}$$

Setting $\beta_1 = 0.0$ (one of the phase angles can be arbitrarily chosen) and taking into consideration the following simplification $\Phi_i + 0.25\Phi_i^3 \approx \Phi_i$, Eq. (24) can be rewritten as

$$W_1^{SYN} = -\frac{m_1 l^2 \alpha^4 \pi \Phi_1}{k_x - \alpha^2 U} m_2 \Phi_2 \sin\beta_2 = W^{SYN},$$
$$W_2^{SYN} = \frac{m_2 l^2 \alpha^4 \pi \Phi_2}{k_x - \alpha^2 U} m_1 \Phi_1 \sin\beta_2 = -W^{SYN}. \tag{25}$$

Equation (25) shows that both synchronization energies are equal and so the energy balance of both pendulums (Eq. (18)) can be written as

$$W_1^{DRIV} = W_1^{DAMP} + W^{SYN}$$
$$W_2^{DRIV} + W^{SYN} = W_2^{DAMP}. \tag{26}$$

Substituting Eqs. (15) and (16) and (25) into Eq. (26) one gets

$$2M_{N1}\gamma_N = \pi\alpha c_{\varphi 1}\Phi_1^2 - \frac{m_1 l^2 \alpha^4 \pi \Phi_1}{k_x - \alpha^2 U} m_2 \Phi_2 \sin\beta_2,$$
$$2M_{N2}\gamma_N = \pi\alpha c_{\varphi 2}\Phi_2^2 + \frac{m_2 l^2 \alpha^4 \pi \Phi_2}{k_x - \alpha^2 U} m_1 \Phi_1 \sin\beta_2, \tag{27}$$

so

$$\sin\beta_2 = \frac{2M_{N2}\gamma_N - \pi\alpha c_{\varphi 2}\Phi_2^2}{\frac{m_2 l^2 \alpha^4 \pi \Phi_2}{k_x - \alpha^2 U} m_1 \Phi_1}. \tag{28}$$

Equations (27) and (28) give relation between the pendulums amplitudes Φ_1 and Φ_2 and the phase angle β_2.

C. Energy dissipated by the c_x-damper

Energy dissipated by the c_x–damper during the period of system oscillations is given by

$$W_b^{DAMP} = \int_0^T c_x \dot{x}^2 dt. \tag{29}$$

Assuming the harmonic oscillations of the beam M which are characterized by the amplitude X, i.e.,

$$x = X\sin(\alpha t + \vartheta), \quad \dot{x} = \alpha X \cos(\alpha t + \vartheta), \tag{30}$$

where ϑ is a phase angle, which determines the phase shift of the beam motion in respect of first pendulum (with phase angle β_1). Comparing Eqs. (8) and (30), assuming $\beta_1 = 0$ and taking into consideration, only first harmonic one gets following formula:

$$\vartheta = \arctan\left(\frac{X_{12}}{X_{11} + X_{12}\cos\beta_2}\right).$$

Substituting Eq. (30) into Eq. (29) one gets

$$W_b^{DAMP} = \int_0^T c_x \dot{x}^2 dt = c_x \alpha \pi X^2. \tag{31}$$

D. The case of the small damping of the pendulums

Let us consider the particular case when the damping of the pendulums is small, i.e., $c_{\varphi i}$ are small, and such is the moment generated by the escapement mechanism. We have

$$\frac{W_1^{DRIV}}{W^{SYN}} \approx 0.0, \quad \frac{W_2^{DRIV}}{W^{SYN}} \approx 0.0,$$
$$\frac{W_1^{DAMP}}{W^{SYN}} \approx 0.0, \quad \frac{W_1^{DAMP}}{W^{SYN}} \approx 0.0. \tag{32}$$

Taking into consideration Eqs. (27) and (32), Eq.(26) has the form

$$W_1^{SYN} = \frac{-m_1 l^2 \alpha^4 \pi \Phi_1}{k_x - \alpha^2 U} m_2 \Phi_2 \sin\beta_2 = 0.0,$$
$$W_2^{SYN} = \frac{m_2 l^2 \alpha^4 \pi \Phi_2}{k_x - \alpha^2 U} m_1 \Phi_1 \sin\beta_2 = 0.0. \tag{33}$$

Equations (33) are fulfilled in two cases: (i) $\beta_2 = 0.0°$, so as $\beta_1 = 0.0°$ indicates the state of complete synchronization, pendulums behave exactly in the same way and there is no transfer of energy between them and (ii) $\beta_2 = 180.0°$, so as $\beta_1 = 0.0°$ indicates the state of antiphase synchronization.

IV. NUMERICAL RESULTS AND DISCUSSION

A. Synchronization of two identical pendulums

In our numerical simulations, Eqs. (1) and (2) have been integrated by the Runge-Kutta method. The initial conditions have been set as follows: (i) for the beam $x(0) = \dot{x}(0) = 0$, (ii) for the pendulums the initial conditions $\varphi_1(0), \dot{\varphi}_1(0)$ have been calculated from the assumed initial phase differences β_1 and β_2 (in all calculations $\beta_1 = 0$ has been taken) using Eq. (3), i.e., $\varphi_1(0) = 0$, $\dot{\varphi}_1(0) = \alpha\Phi$, $\varphi_2(0) = \Phi\sin\beta_2$, $\dot{\varphi}_2(0) = \alpha\Phi\cos\beta_2$. Stability of the obtained synchronous states has been investigated using the variational equations as described in (Czolczynski *et al.*, 2009a,b).

Depending on initial conditions, one can observe two different types of synchronization in the considered system. Two pendulums with identical masses and periods of oscillations can obtain the state of complete synchronization when ($\varphi_1 = \varphi_2$) and beam M oscillates in antiphase to the pendulums or the state of antiphase synchronization when ($\varphi_1 = -\varphi_2$) and beam M is at rest (Blekhman, 1988; Bennet, *et al.*, 2002; Czolczynski *et al.*, in press).

Both types of synchronization are shown in Figures 2(a)–2(c). In our numerical simulations, we consider the following parameter values: pendulums' masses—$m_1 = m_2 = 1.0$ [kg], the length of the pendulums $l = g/4\pi^2 = 0.2485$ [m] (it has been selected in such a way when the beam M is at rest period of pendulum oscillations is equal to $T = 1.0$ [s] and oscillations frequency to $\alpha = 2\pi$ [s^{-1}]), $g = 9.81$ [m/s^2] is an acceleration due to the gravity, beam mass $M = 10.0$ [kg], damping coefficients $c_{\varphi 1} = c_{\varphi 2} = 0.0083$ [Ns] and $c_x = 1.53$ [Ns/m], and stiffness coefficient $k_x = 4.0$ [N/m]. When the displacements of the pendulums are smaller than $\gamma_N = 5.0°$, escapement mechanisms generate driving moments $M_{N1} = M_{N2} = 0.075$ [Nm], allow pendulums to oscillate with amplitude $\Phi_1 = \Phi_2 = \Phi = 0.2575$ ($\approx$14.75°) when beam M is at rest.

Figure 2(a) presents the complete synchronization of the pendulums of both clocks, i.e., pendulums' displacements are the same $\varphi_1 = \varphi_2$ and the displacements of the beam x (shown in 10 times magnification). The time series are shown

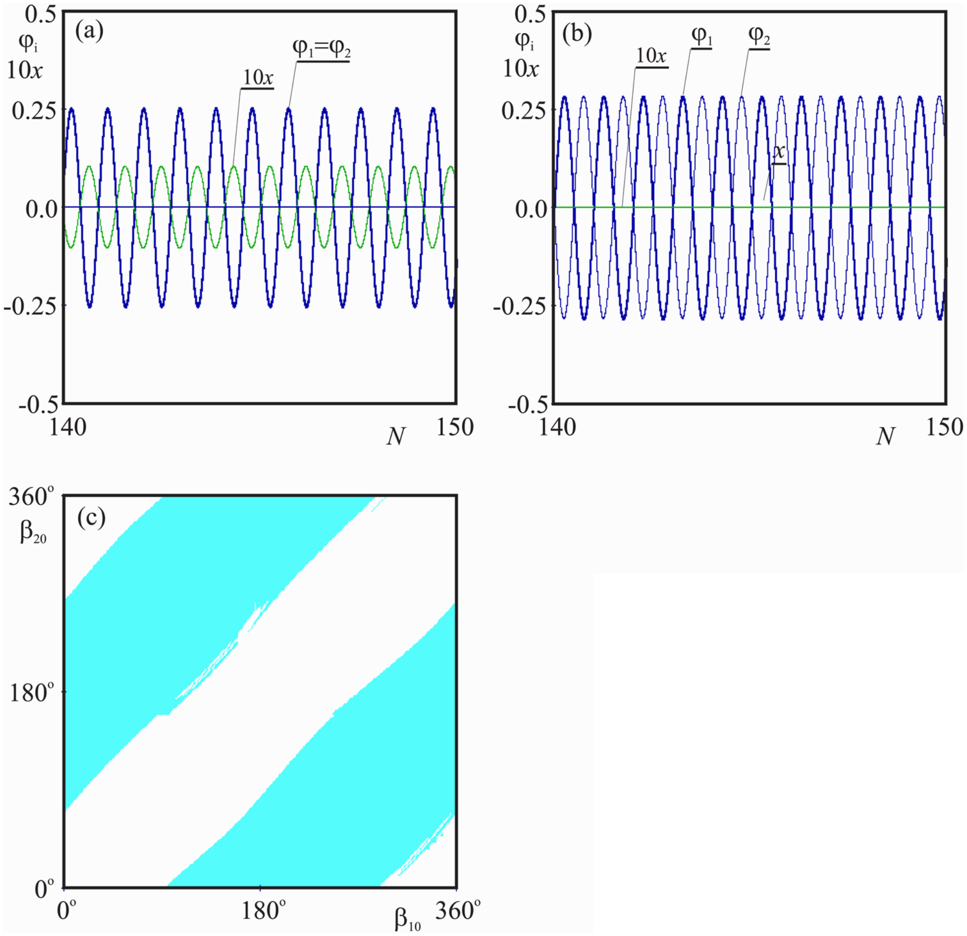

FIG. 2. (Color online) Synchronization of two identical pendulum clocks': $m_1 = m_2 = 1.0$ [kg], $l = g/4\pi^2 = 0.2485$ [m], $M = 10.0$ [kg], $c_{\varphi 1} = c_{\varphi 2} = 0.0083$ [Ns], $c_x = 1.53$ [Ns/m], $k_x = 4.0$ [N/m], $\gamma_N = 5.0°$, $M_{N1} = M_{N2} = 0.075$ [Nm]; (a,b) time series of pendulums φ_1, φ_2 and beam x displacements, time on the horizontal axis is given in the following way $t = NT$, where $N = 1,2,3,\ldots$ and $T = 1$[s], (a) complete synchronization ($\varphi_1 = \varphi_2$) pendulums are in antiphase to the oscillations of the beam M, (b) anti-phase synchronization ($\varphi_1 = -\varphi_2$), beam M is at rest, (c) basins of attraction of complete synchronization (white color) and antiphase synchronization (gray color, blue color online) in β_{10}-β_{20} plane, $x(0) = 0.0$, $\dot{x}(0) = 0.0$, $\varphi_{i0} = \Phi \sin\beta_{i0}$, $\dot{\varphi}_{i0} = \alpha\Phi\cos\beta_{i0}$.

in stationary state after the decay of transients. Time on the horizontal axis is given in the following way $t = NT$, where $N = 1,2,3,\ldots$ and T is a period of pendulum's oscillations when the beam is at rest. Notice that the numerically estimated value of the amplitude $\Phi_{1,2} = 0.283$ is approximately equal to the value calculated from Eq. (21). In Figure 2(b), we present the example of antiphase synchronizations, i.e., $\varphi_1(t) = \varphi_2(t + 0.5T)$ (or $\varphi_1(t) = -\varphi_2(t)$) and the beam M is at rest as $x = 0.0$. Both types of synchronization have been obtained for the same parameter values but different initial conditions. Figure 2(c) shows the basins of attraction of both types of synchronization in the (β_{10}, β_{20}) plane. White and grey (blue online) colors indicate initial conditions leading, respectively, to complete and antiphase synchronization. In the case of complete synchronizations, both clocks are significantly faster (nearly 6 minutes per hour – Figure 2(a)) with reference to the clock mounted to the nonmoving base. This difference occurs as the result of the pendulums' motion in antiphase to the beam. In the case of antiphase synchronization (Figure 2(b)), the clocks remain accurate.

B. Synchronization of two pendulums with different masses

When the clocks have pendulums with different masses ($m_1 \neq m_2$), the considered system shows three different types of synchronous behavior. The first one is the complete synchronization ($\varphi_1 = \varphi_2$) already observed in the case of identical systems in Sec. A. The second one is the phase synchronization which evolves from the anti-phase synchronization of the identical systems. For nonidentical masses of the pendulums, the phase difference between pendulums decreases and is smaller than π (180°) and contrary to the case of identical clocks the beam M is not at rest and pendulums' amplitudes are not equal.

Different types of synchronization states and their basins of attraction are presented in Figures 3(a)–3(d). In our numerical simulations, we consider the following parameter values: $l = g/4\pi^2 = 0.2485$ [m], $M = 10.0$ [kg], $c_x = 1.53$ [Ns/m], $k_x = 4.0$ [N/m], $m_1 = 1.0$ [kg], $m_2 = 2.65$ [kg], $\gamma_N = 5.0°$, $c_{\varphi 1} = 0.0083$ [Ns], $c_{\varphi 2} = 0.0083 \times m_2$ [Ns], $M_{N1} = 0.075$ [Nm], and $M_{N2} = 0.075 \times m_2$ [Nm]. Figure 3(a) presents the phase synchronization in which the pendulums' displacements φ_1 and φ_2 are shifted by the angle close to π but smaller than this value. Similarly, the oscillations of the beam x are phase shifted to the pendulums' oscillations by the value close but not equal to $\pi/2$. The first pendulum (with smaller mass m_1) exhibits the oscillations with the larger amplitude (than in the case when beam M is at rest). The analysis of Sec. III explains this phenomenon showing that this pendulum is driven by the second pendulum via beam M (the part of pendulum 2 energy is transferred to pendulum 1). As the result, the amplitude of the second pendulum's oscillations decreases.

In the considered system besides the complete and phase synchronization, one can observe the synchronization state in which φ_1–φ_2 is a periodic function. As the period of this

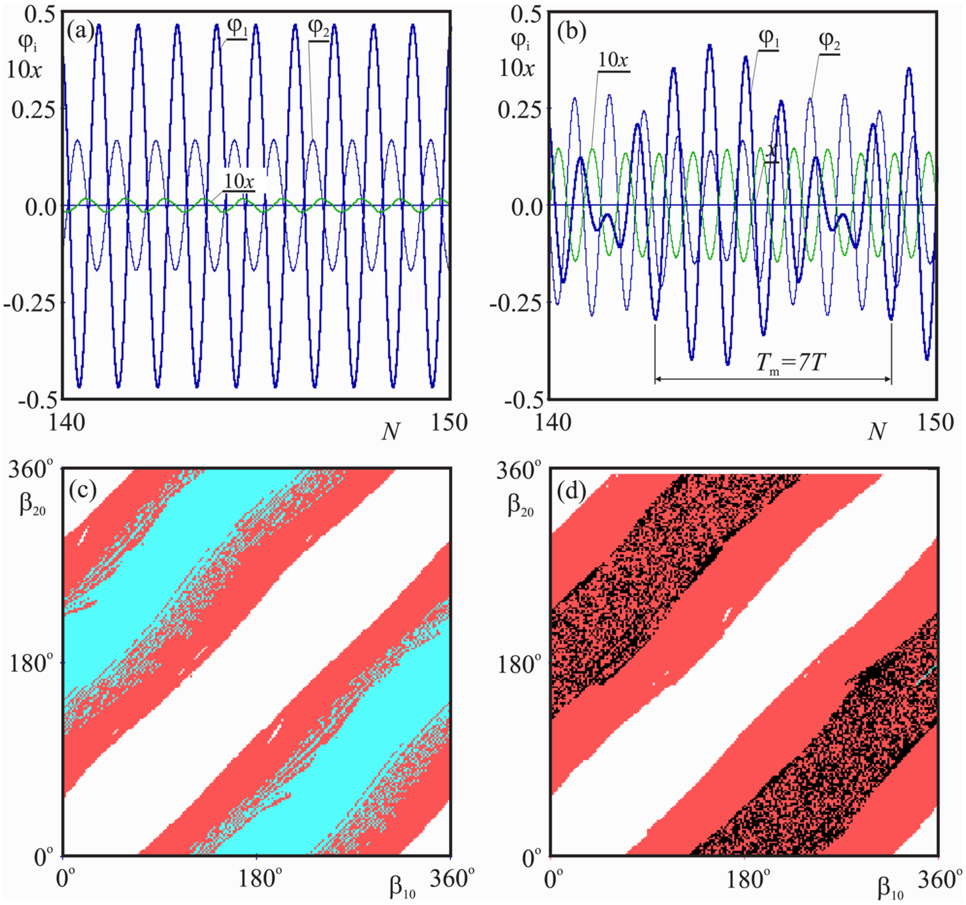

FIG. 3. (Color online) Synchronization of two pendulums with different masses: $m_1 = 1.0$ [kg], $l = g/4\pi^2 = 0.2485$ [m], $M = 10.0$ [kg], $c_x = 1.53$ [Ns/m], $k_x = 4.0$ [N/m], $\gamma_N = 5.0°$, $c_{\varphi 1} = 0.0083$ [Ns], $c_{\varphi 2} = 0.0083 \times m_2$ [Ns], $M_{N1} = 0.075$ [Nm], $M_{N2} = 0.075 \times m_2$ [Nm]; (a) and (b) time series of pendulums φ_1, φ_2 and beam x displacements, time on the horizontal axis is given in the following way $t = NT$, where $N = 1,2,3,\ldots$ and $T = 1$[s], (a) phase synchronization: $m_2 = 2.65$ [kg], $\beta_{10} = 10°$, $\beta_{20} = 130°$; (b) long period synchronization: $m_2 = 2.65$ [kg], $T_m \approx 7T$, $\beta_{10} = 1°$, $\beta_{20} = 90°$; (c) basins of attraction of different types of synchronization: complete synchronization (white), phase synchronization (light grey, blue color online), long period synchronization (dark gray, red color online) in β_{10}-β_{20} plane: $x(0) = 0.0$, $\dot{x}(0) = 0.0$, $\varphi_{i0} = \Phi \sin \beta_{i0}, \dot{\varphi}_{i0} = \alpha\Phi \cos \beta_{i0}$, $m_2 = 2.65$ [kg], (d) basins of attraction of different types of synchronization: complete synchronization (white), long period synchronization (dark gray, red color online) chaotic behavior (black) in β_{10}-β_{20} plane: $x(0) = 0.0$, $\dot{x}(0) = 0.0$, $\varphi_{i0} = \Phi \sin \beta_{i0}$, $\dot{\varphi}_{i0} = \alpha\Phi \cos \beta_{i0}$, $m_2 = 3.105$ [kg].

function T_m is larger than T (the period of pendulums' oscillations in the case when beam M is at rest), this type of generalized synchronization is called a long period synchronization. (The long period synchronization can be a special case of $n{:}m$ synchronization observe in the self-excited continuous systems. Since the system (1-2) is discontinuous and we have not proved the existence of the quasiperiodic solution on the torus in it we decide to use other name.) Figure 3(b) presents the example of this type of synchronization obtained for the initial conditions $\beta_{10} = 1.0°$ and $\beta_{20} = 90.0°$. One can observe that T_m is equal to $7T$. Long period synchronization can be explained by the periodic decrease of the amplitude Φ_1 of the pendulum 1 oscillations. When this amplitude is smaller than the minimum value $\Phi_1 = \gamma_N$, the escapement mechanism is switched. These switches off introduce the perturbation to the system. The basins of attraction of three coexisting attractors are shown in Figure 3(c) in β_{10}–β_{20} plane. White and light gray (blue online) colors indicate initial conditions leading respectively to complete and antiphase synchronization while the region shown in dark gray (red online) color indicates initial conditions leading to long period synchronization. Our calculations show that the dark gray basin of long period synchronization appears at $m_2 \approx 2.4$ [kg]. With the increase of m_2 the basin of phase synchronization becomes smaller and it finally disappears for $m_2 \approx 2.8$ [kg]. In the considered system, we observed long period synchronization states with different T_m (the largest observed T_m is equal to $51T$). Long period synchronization can coexist with the chaotic behavior of the clocks' pendulums. (This type of clocks' behavior is the topic of our current studies. It has been shown that the system can be chaotic as the largest Lyapunov exponent estimated by the synchronization method (Stefanski and Kapitaniak, 2003) is positive. Additionally we observe the co-existence of the different chaotic and long period synchronization states with very small basins of attraction. Details of this results will be published elsewhere. Chaotic behavior of the pendulum clock is also predicted and described in Moon and Stiefel (2006) but model of the clock has been used.) The example of such a coexistence is shown in Figure 3(d) ($m_2 = 3.105$ [kg]) where the basins of complete (white color), long period with $T_m = 13T$ (dark gray, red online) synchronization and chaotic behavior (black color) are shown.

In the case of phase synchronization both clocks are slightly slower (nearly 20 [s] per hour – Figure 3(a)) in reference to the clock mounted to the nonmoving base. The same difference occurs in the case of long period synchronization (25 [s] per hour – Figure 3(b)).

In Figures 4(a)–4(c) we present the bifurcation diagram of the system (1,2). The mass of pendulum 2-m_2 has been taken as a control parameter. On the vertical axis, the displacements of the pendulums φ_1, φ_2 the beam displacement x (for better visibility x has been multiplied by 10); values φ_2 and x have been taken at the time of maximum values of φ_1, i.e., when $\dot{\varphi}_1$ changes the sign from positive to negative values. In Figures 4(a) and 4(b), the bifurcation diagrams for, respectively, increasing and decreasing values of m_2 are shown. In Figure 4(a), we start from the antiphase synchronization of identical systems (i.e., $m_2 = 1.0$ [kg]). The antiphase

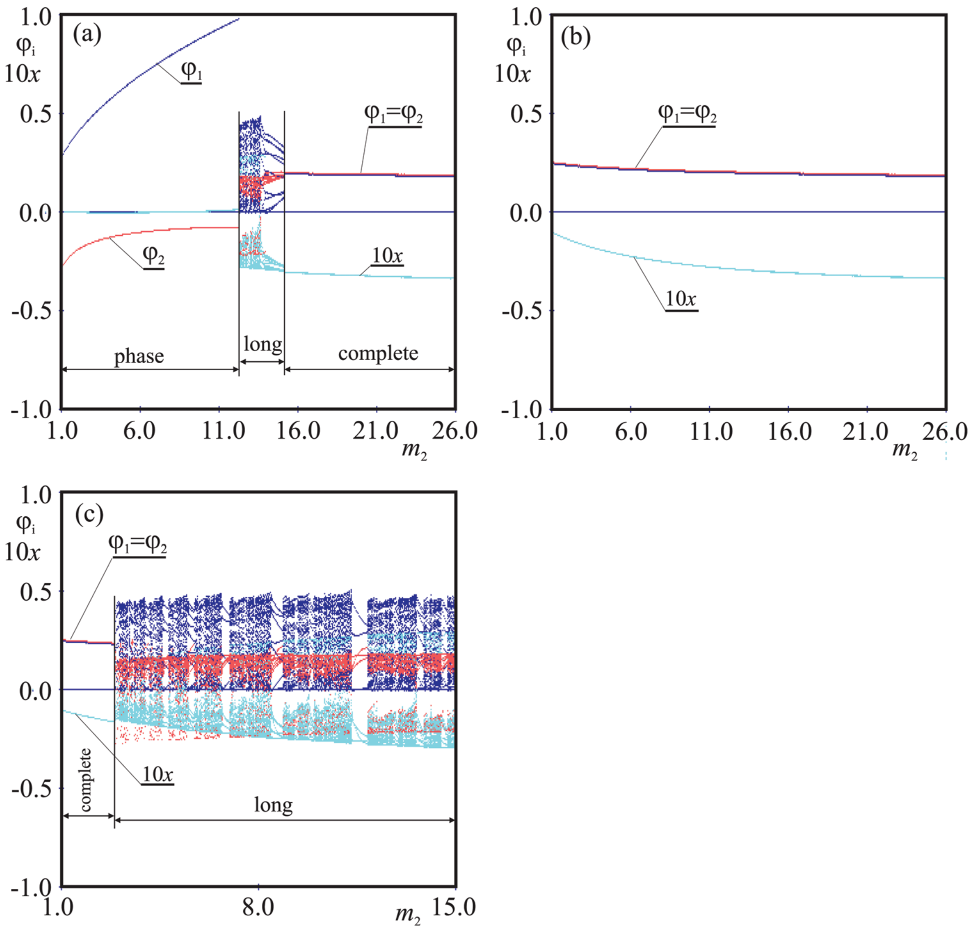

FIG. 4. (Color) Bifurcation diagrams of system (1,2): φ_1, φ_2 and x versus control parameter m_2: $\Phi_1 \approx \gamma_N = 5.0°$, $m_1 = 1.0$ [kg], $l = g/4\pi^2 = 0.2485$ [m], $M = 10.0$ [kg], $c_x = 1.53$ [Ns/m], $k_x = 3.94$ [N/m], $\gamma_N = 5.0°$, $c_{\varphi_1} = 0.0083$ [Ns], $c_{\varphi_2} = 0.0083 \times m_2$ [Ns], $M_{N1} = 0.075$ [Nm], $M_{N2} = 0.075 \times m_2$ [Nm]; (a) m_2 increases from 1 to 26.0, (b) m_2 decreases from 26.0 to 1.0, (c) m_2 decreases from 15.0 to 1.0.

synchronization is replaced by the phase synchronization with decreasing phase shift which can be observed in the interval 1.0 [kg]<m_2<12.3 [kg]. For larger values of m_2, one observes long periodic synchronization and chaotic oscillations of the clocks' pendulums (12.3 [kg]<m_2<15.25 [kg]). This behavior is replaced by complete synchronization for m_2>15.25 [kg]. Figure 4(b) shows that starting from the complete synchronization for $m_2 = 26$ [kg] and decreasing the values of m_2 we observe this type of synchronization in the whole interval 1.0 [kg]<m_2<26.0 [kg]. In Figure 4(c), we start from the chaotic oscillations for $m_2 = 15.0$ [kg] and decrease the value of the control parameter m_2. Chaotic oscillations with the windows of long period synchronization are preserved in the interval 2.9 [kg]<m_2<15.0 [kg] and for smaller values of m_2 are replaced by complete synchronization.

Figures 4(a)–4(c) confirms the coexistence of different types of synchronous behavior. For 1.0 [kg]<m_2<2.9 [kg], complete and phase synchronizations coexist. In the interval 2.9 [kg]<m_2<12.3 [kg], we observe complete, phase and long period synchronization (with different n). For larger values of m_2 (12.3 [kg]<m_2<15.25 [kg]), phase synchronization disappears, and we observe complete and long period synchronization. Finally, for m_2>15.25, only the complete synchronization is possible.

The system behavior for m_2 smaller than m_1 is discussed in Figures 5(a) and 5(b). Bifurcation diagram is presented in Figure 5(a) where we start from the phase synchronization for $m_2 = 1.0$ [kg] and decrease the value of control parameter up to $m_2 = 0.1$ [kg]. Phase synchronization is preserved in the interval 1.0 [kg]>m_2>0.285 [kg] (it coexists with complete synchronization). For smaller values of m_2, we observe the complete synchronization only. The disappearance of the phase synchronization is explained in Figure 5(b) where we present the time series of the pendulums' displacements φ_1 and φ_2 for $m_2 = 0.285$ [kg] (close to the threshold value). Notice that the amplitude of pendulum 1 is only slightly larger that $\gamma_N = 5.0°$. Further decrease of m$_2$ results in the switch off of the escapement mechanism and allows the transition to the complete synchronization. For m_2<m_1, long period synchronization has not been observed. Notice that in Figure 5(b), the phase shift β_2 between pendulums' displacements is smaller than 180.0° and approximately equal to 126°. Similarly, as in the example of Figure 3(a), the difference in the pendulums' amplitudes is created by the energy transfer from pendulum 1 to pendulum 2, as described in Sec. III in Eq.(26).

To explain why the antiphase synchronization of the identical clocks is replaced by the phase synchronization of nonidentical ones, let us consider the energy balance of the synchronized states shown in Figures 6(a) and 6(b).

In the case of antiphase synchronization of identical pendulums (Figure 6(a)), we have two independent streams of energy (both fulfill Eq. (19)), as both pendulums dissipate the same amount of energy as they gain from the escapement

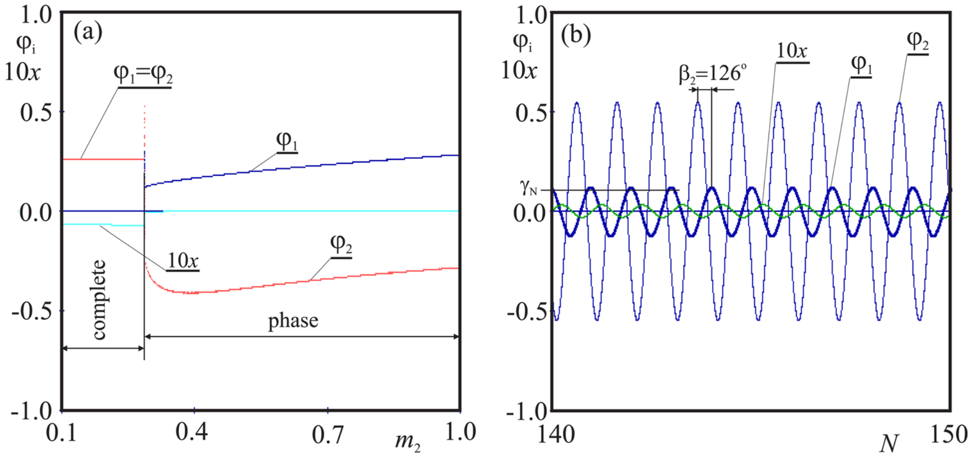

FIG. 5. (Color online) (a) Bifurcation diagram of system (1,2): φ_1, φ_2 and x versus control parameter m_2; m_2 decreases from 1.0 [kg] to 0.1 [kg], (b) time series of φ_1, φ_2 and x during the phase synchronization: $\Phi_1 \approx \gamma_N = 5.0°$ $m_1 = 1.0$ [kg], $l = g/4\pi^2 = 0.2485$ [m], $M = 10.0$ [kg], $c_x = 1.53$ [Ns/m], $k_x = 3.94$ [N/m], $\gamma_N = 5.0°$, $c_{\varphi_1} = 0.0083$ [Ns], $c_{\varphi_2} = 0.0083 \times m_2$ [Ns], $M_{N1} = 0.075$ [Nm], $M_{N2} = 0.075 \times m_2$ [Nm].

mechanism. In Figure 6(b), we presented the energy balance of the pendulums with different masses in the state of phase synchronization. We consider the parameter values of Figure 5(b) and numerically calculated pendulum's amplitudes $\Phi_1 = 0.121$ and $\Phi_2 = 0.548$. The streams fulfill Eq. (26). The W_1^{DRIV} transferred to the first pendulum (one with smaller amplitude) is divided in to the energy dissipated in the damper c_{φ_1} and energy W^{SYN} transferred to the second pendulum. Notice that the phase shift β_2 calculated from Eq. (28) is approximately the same as the numerically calculated value $\beta_2 = 126°$ (see Figure 5(b)). Eqs. (15), (16), and (25) allow estimation of the energies: W_i^{DRIV}, W_i^{DAMP}, and W_i^{SYN}. The comparison of analytical and numerical results is presented in Table I.

The differences between analytical and numerical results are small (values W_1^{DRIV} and W_2^{DRIV} are exact) what confirm the accuracy of our energy balance approach. The value of $W_b^{DAMP} = 0.00029$ [Nm] is significantly smaller than the values of other energies and is not considered in Figures 6(a) and 6(b) and Table I.

The analytical studies of Secs. II and III are based on the assumption that the periods of pendulums' oscillations are constant and equal to $2\pi/\alpha$. When clocks are coupled via a movable beam pendulums' periods are not constant and depend on the pendulums' masses, the variations of this period are small (for example, smaller than 5% for the $m_2/m_1 = 11$ and parameters of Table I).

V. CONCLUSIONS

We consider the synchronization of two clocks which have pendulums with the same length but different masses. As both pendulums have the same length both clocks are accurate, i.e., they show the same time. We show that two such clocks hanging on the same beam can synchronize both in-phase and anti-phase as has already been shown in Blekham (1988), Bennet et al. (2002), and Czolczynski et al. (in press), but contrary to that results we show that the third type of synchronization in which the difference of the pendulums' displacements φ_1-φ_2 is a periodic function of time. This period T_m is larger than T (the period of pendulums' oscillations in the case when beam M is at rest) p times, where p is the integer dependent on the clock's parameters. We call this type of generalized synchronization a long period synchronization. Long period synchronization coexists with the chaotic behavior in which the oscillations of the clocks' pendulums are uncorrelated and unpredictable.

Our approximate analytical analysis allows deriving the synchronizations conditions which explain the observed types of synchronizations and give formula for both the

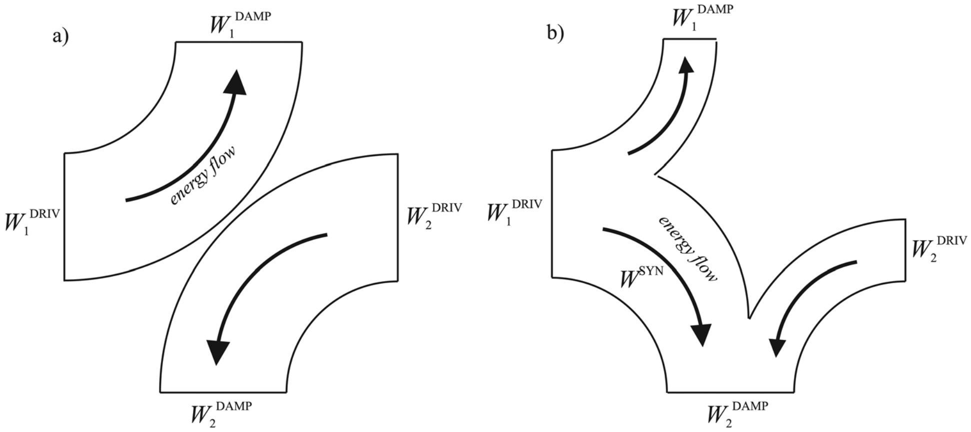

FIG. 6. Energy balance of pendulums: (a) antiphase synchronization of identical pendulums – there is no transfer of energy between pendulums, (b) phase synchronization of the pendulums with different masses: $m_1 = 1.0$ [kg] and $m_2 = 0.289$ [kg] and $\Phi_1 \approx \gamma_N = 5.0°$– pendulum 1 transfer energy to the pendulum 2 via the beam M.

TABLE I. Comparison of analytical and numerical results: $m_1 = 1.0$ [kg], $m_2 = 0.289$ [kg], $l = g/4\pi^2 = 0.2485$ [m], $M = 10.0$ [kg], $c_x = 1.53$ [Ns/m], $k_x = 3.94$ [N/m], $\gamma_N = 5.0°$, $c_{\varphi 1} = 0.0083$ [Ns], $c_{\varphi 2} = 0.0083 \times m_2$ [Ns], $M_{N1} = 0.075$ [Nm], $M_{N2} = 0.075 \times m_2$ [Nm].

	Numerical	Analytical
$W_1{}^{SYN}$	$W_1^{SYN} = \int_0^T m_1 \ddot{x} l \cos\varphi_1 \dot{\varphi}_1 dt = -0.0101[Nm]$	$W_1^{SYN} = -W_2^{SYN}$
$W_2{}^{SYN}$	$W_2^{SYN} = \int_0^T m_2 \ddot{x} l \cos\varphi_2 \dot{\varphi}_2 dt = 0.0100[Nm]$	$W_2^{SYN} = \frac{2m_2 l^2 \alpha^4 \pi \Phi_1}{k_x - \alpha^2 U} m_2 \Phi_2 \sin\beta_2 = 0.0107[Nm].$
$W_1{}^{DRIV}$	$W_1^{DRIV} = 2M_{N1}\gamma_N = 0.0131[Nm]$	$W_1^{DRIV} = 2M_{N1}\gamma_N = 0.0131[Nm]$
$W_2{}^{DRIV}$	$W_2^{DRIV} = 2M_{N2}\gamma_N = 0.0036[Nm]$	$W_2^{DRIV} = 2M_{N2}\gamma_N = 0.0036[Nm]$
$W_1{}^{DAMP}$	$W_1^{DAMP} = \int_0^T c_{\varphi 1}\dot{\varphi}_1^2 dt = 0.0028[Nm]$	$W_1^{DAMP} = \pi\alpha c_{\varphi 1}\Phi_1^2 = 0.0024[Nm]$
$W_2{}^{DAMP}$	$W_2^{DAMP} = \int_0^T c_{\varphi 2}\dot{\varphi}_2^2 dt = 0.0137[Nm]$	$W_2^{DAMP} = \pi\alpha c_{\varphi 2}\Phi_2^2 = 0.0143[Nm]$

pendulums' amplitudes and phase shift between them. The consideration of the energy balance in the system allows showing the pendulum of the smaller mass transfer part of its energy (gained through the escapement mechanism) to the other pendulum via the oscillating beam.

In the synchronized state the clocks are not accurate (the exception is the antiphase synchronization of the identical clock when the beam is at rest). In the case of complete synchronization, the clocks are significantly faster (in reference to the clock mounted to the nonmoving base) as the result the pendulums motion in antiphase to the beam. In the case of phase synchronization and long period synchronizations, the clocks are slightly slower.

ACKNOWLEDGMENT

This work has been supported by the Foundation for Polish Science, Team Programme – Project No TEAM-2010/5/5. P.P. acknowledges the support from Foundation for Polish Science (the START fellowship).

Andronov, A., Witt, A., and Khaikin, S., *Theory of Oscillations* (Pergamon, Oxford, 1966).

Bennet, M., Schatz, M. F., Rockwood, H., and Wiesenfeld, K., "Huygens's clocks," Proc. R. Soc. London, Ser. A **458**, 563 (2002).

Blekham, I. I., *Synchronization in Science and Technology* (ASME, New York, 1988).

Huygens, C., *Horoloqium Oscilatorium* (Apud F. Muquet, Parisiis, 1673); English translation: *The Pendulum Clock* (Iowa State University Press, Ames, 1986).

Huygens, C., "Letter to de Sluse, In: Oeuveres Completes de Christian Huygens" (letters; no. 1333 of 24 February 1665, no. 1335 of 26 February 1665, no. 1345 of 6 March 1665) (Societe Hollandaise Des Sciences, Martinus Nijhoff, La Haye, 1893).

Czolczynski, K., Perlikowski, P., Stefanski, A., and Kapitaniak, T., "Clustering of Huygens' clocks," Prog. Theor. Phys. **122**, 1027 (2009a).

Czolczynski, K., Perlikowski, P., Stefanski, A., and Kapitaniak, T., "Clustering and synchronization of Huygens' clocks," Physica A **388**, 5013 (2009b).

Czolczynski, K., Perlikowski, P., Stefanski, A., and Kapitaniak, T., "Huygens' odd sympathy experiment revisited," Int. J. Bifurcation Chaos Appl. Sci. Eng. (in press).

Dilao, R., "Antiphase and in-phase synchronization of nonlinear oscillators: The Huygens's clocks system," Chaos **19**, 023118 (2009).

Fradkov, A. L., and Andrievsky, B., "Synchronization and phase relations in the motion of two pendulum system," Int. J. Non-linear Mech. **42**, 895 (2007).

Kumon, M., Washizaki, R., Sato, J., Mizumoto, R. K. I., and Iwai, Z., "Controlled synchronization of two 1-DOF coupled oscillators," in *Proceedings of the 15th IFAC World Congress*, Barcelona, 2002.

Lepschy, A. M., Mian, G. A., and Viaro, U., "Feedback control in ancient water and mechanical clocks," IEEE Trans. Educ. **35**, 3 (1993).

Moon, F. C., and Stiefel, P. D., "Coexisting chaotic and periodic dynamics in clock escapements," Phil. Trans. R. Soc. A **364**, 2539 (2006).

Pantaleone, J., "Synchronization of metronomes," Am. J. Phys. **70**, 992 (2002).

Pikovsky, A., Roesenblum, M., and Kurths, J., *Synchronization: An Universal Concept in Nonlinear Sciences* (Cambridge University Press, Cambridge, 2001).

Pogromsky, A. Yu., Belykh, V. N., and Nijmeijer, H., "Controlled synchronization of pendula," in *Proceedings of the 42nd IEEE Conference on Design and Control*, Maui, Hawaii, 2003, pp. 4381–4385.

Roup, A. V., Bernstein, D. S., Nersesov, S. G., Haddad, W. S., and Chellaboina, V., "Limit cycle analysis of the verge and foliot clock escapement using impulsive differential equations and Poincare maps," Int. J. Control **76**, 1685 (2003).

Rowlings, A. L., *The Science of Clocks and Watches* (Pitman, New York, 1944).

Senator, M., "Synchronization of two coupled escapement-driven pendulum clocks," J. Sound Vib. **291**, 566 (2006).

Stefanski and T. Kapitaniak, "Estimation of the dominant Lyapunov exponent of non-smooth systems on the basis of maps synchronization," Chaos, Solitons Fractals **15**, 233 (2003).

Ulrichs, H., Mann, A., and Parlitz, U., "Synchronization and chaotic dynamics of coupled mechanical metronomes," Chaos **19**, 043120 (2009).